**SCIENTIFIC COMMITTEE**
**TWENTY-SECOND REGULAR SESSION**
11-19 August 2026
Apia, Samoa (Hybrid)

# NEW AGE-AT-LENGTH DATA FOR WCPO BIGEYE AND YELLOWFIN TUNA FROM THE TEMPERATE NORTH PACIFIC AND APPROACHES TO ADDRESS SPATIAL SAMPLING BIAS IN GROWTH ESTIMATION WITHIN MFCL

**WCPFC-SC22-2026-SA-IP08**
**14 July 2026**

**Submitted by**

**Takaaki Hasegawa[1], Kei Okamoto[1], Hirotaka Ijima[1], Kyuhan Kim[2], Paul Hamer[2], Corey Wakefield[2], Alexander Pons[2], Joseph Widdrington[2] and Nick Davies[3]**

[1] Fisheries Research and Education Agency, Fisheries Resources Institute, Yokohama, Japan
[2] Oceanic Fisheries Programme(OFP), Pacific Community (SPC), Nouméa, New Caledonia
[3] Te Takina Ltd, Whangarei, New Zealand

# New age-at-length data for WCPO bigeye and yellowfin tuna from the temperate North Pacific and approaches to address spatial sampling bias in growth estimation within MFCL

Takaaki Hasegawa[1], Kei Okamoto[1], Hirotaka Ijima[1], Kyuhan Kim[2], Paul Hamer[2], Corey Wakefield[2], Alexander Pons[2], Joseph Widdrington[2] and Nick Davies[3]

[1] Fisheries Research and Education Agency, Fisheries Resources Institute, Yokohama, Japan

[2] Oceanic Fisheries Programme(OFP), Pacific Community (SPC), Nouméa, New Caledonia

[3] Te Takina Ltd, Whangarei, New Zealand

## Summary

- Existing otolith datasets used in the WCPO stock assessments for BET and YFT have been predominantly collected from tropical and subtropical waters south of 10°N, which may not adequately represent growth across the entire assessment domain.
- To address this sampling gap, we collected and aged otolith samples from the temperate North Pacific (N = 443 for BET, N = 141 for YFT). Comparison of growth curves estimated separately from temperate (JPN) and tropical/sub-tropical (SPC) samples revealed marked differences in estimated parameters for BET, with higher Linf and lower k in the temperate area (Linf = 178 cm, k = 0.30 $yr^{-1}$) than the tropical area (Linf = 150 cm, k = 0.38 $yr^{-1}$). Although this comparison is only indicative as the JPN data set does not cover the lower part of the length range (<60 cm FL) that is covered in the SPC data set.
- Because MFCL assumes a single growth curve across the entire assessment domain, simply combining both otolith datasets can introduce bias in the estimated growth curve. If the regional composition of the conditional age-at-length (CAAL) data does not reflect the actual distribution of the stock, regions with low abundance but dense sampling will disproportionately influence the estimated growth curve. To address this issue, regions with a higher relative mean density should contribute more CAAL observations to the growth estimate.
- We propose two approaches that use CPUE as a proxy for regional relative abundance: Approach 1) resampling otolith observations with probability proportional to CPUE prior to model input, correcting the regional composition of the CAAL dataset itself; Approach 2) applying region-specific scalars (λr) to the observed sample size of CAAL data within MFCL, where λr is derived from the mean CPUE within each model region.
- We make the following two recommendations.
    1. The new age-at-length data collected from the temperate North Pacific be included in the 2026 BET and YFT stock assessments.

2. One of the proposed weighting approaches be evaluated as a sensitivity analysis in the 2026 WCPO BET stock assessment.

## Introduction

Stock assessments of bigeye tuna (BET, *Thunnus obesus*) and yellowfin tuna (YFT, *Thunnus albacares*) in the western and central Pacific Ocean (WCPO) are conducted using MULTIFAN-CL (MFCL; Day et al. 2023; Magnusson et al. 2023), a size-, age-, and spatially-structured integrated stock assessment model. Growth is one of the key biological processes in MFCL because it determines the relationship between age and length within the population and directly influences estimates of selectivity, biomass, and fishing mortality. Consequently, misspecification of growth can propagate throughout the assessment and substantially affect estimates of stock status and management quantities (Punt et al. 2015; Correa et al. 2021). In current WCPO BET and YFT assessments, the von Bertalanffy (VB) growth curve is estimated internally within MFCL using both conditional age-at-length (CAAL) data and size composition data, with CAAL data derived from otolith-based age estimates providing the primary source of direct information on growth. However, the available CAAL dataset is dominated by samples collected from tropical and subtropical waters south of 10°N (Farley et al. 2020), while the temperate North Pacific remains poorly represented. This spatial imbalance in otolith sampling may reduce the representativeness of the growth curve estimated for the entire assessment domain.

Another important issue is that MFCL assumes a single growth curve across the entire assessment domain and does not account for spatial variation in growth. Previous work has suggested that BET growth may vary among regions within the WCPO (Farley et al. 2017). If such regional differences exist, a single growth curve estimated from pooled CAAL data represents an average of multiple regional growth patterns. Under this framework, the estimated growth curve is influenced by the geographic composition of the CAAL dataset. Consequently, regions contributing more CAAL observations will have a greater influence on the estimated growth curve regardless of their relative contribution to the overall stock. Ideally, the contribution of each region should reflect its relative abundance within the stock rather than the intensity of biological sampling (Peatman et al. 2025). However, no established approach currently exists to account for regional abundance when estimating growth within MFCL-based tuna assessments.

To address these issues, we present new otolith data from the temperate North Pacific and evaluate two approaches for estimating a growth curve that better reflects the spatial distribution of the stock across the assessment region. First, we expand the available CAAL dataset for WCPO BET and YFT by incorporating newly aged otolith samples collected from Japanese fisheries operating in the temperate North Pacific. Second, we evaluate two approaches that use standardized CPUE as a proxy for regional relative abundance: (1) resampling otolith observations with probabilities proportional to CPUE prior to model fitting,

thereby adjusting the regional composition of the CAAL dataset; and (2) applying region-specific scalars (λr) to the observed sample size of CAAL data within MFCL, where λr is derived from the mean CPUE in each model region.

## Materials and Methods

### 2.1.1 Otolith data

A total of 443 BET and 141 YFT otoliths were collected in the subtropical and temperate North Pacific between 2006 and 2024 from Japanese commercial, training, and research vessels. Longline fishery accounted for 93% of BET samples and 77% of YFT samples. Pole-and-line fishery accounted for an additional 5% and 6%, respectively. Sampling locations spanned 10°N–37°N and 128°E–158°W for BET and 10°N–39°N and 124°E–170°W for YFT. Fork length ranged from 60 to 177 cm for BET and from 60 to 145 cm for YFT. Sampling occurred in all four quarters for both species, though BET samples were concentrated in Q1 and Q4 (n=132 and 172, respectively) with fewer in Q3 (n=48). YFT samples were distributed relatively evenly across quarters (Q1–Q4: n=30, 32, 34, 45).

The otoliths were sent to Fish Ageing Services Pty Ltd (FAS; Hobart, Australia) for sectioning and reading. FAS conducted age estimation for the SPC dataset (Farley et al. 2017, 2020), and using the same laboratory ensured methodological consistency between the two datasets. The detailed protocol to estimate the annual age is described in Farley et al. (2017, 2020). In brief, sagittal otoliths were embedded in clear casting polyester resin, and serial transverse sections approximately 300 µm thick were cut through the primordium. Sections were examined at 25× magnification under transmitted light, and opaque zones were counted from the primordium to the otolith edge. A decimal age was estimated for each fish using the method of Farley et al. (2025), incorporating opaque zone counts, otolith measurements, and capture date.

The Japanese dataset was combined with the WCPO CAAL data compiled by SPC for the 2026 BET and YFT stock assessments, which consisted of 1,644 BET and 1,832 YFT otolith samples collected from the tropical and subtropical WCPO (41°S–31°N, 120°E–123°W). Fork length ranged from 14 to 183 cm for BET and from 14 to 174 cm for YFT. The combined dataset included 2,087 BET and 1,973 YFT samples, expanding the spatial coverage of the available CAAL data to include the subtropical and temperate North Pacific.

### 2.1.2 Growth analysis

A VB growth model was fit to the age-at-length data. The VB model takes the form

$$L_t = L_{inf}(1 - e^{-k(t-t_0)})$$

where $L_t$ is the fork length at age $t$, $L_t$ is the mean asymptotic fork length, $k$ is a growth rate coefficient (year$^{-1}$), and $t_0$ is the theoretical age at zero length. Parameters were estimated

by nonlinear least squares using R (R Core Team). Models were fitted separately to the Japanese dataset, the SPC dataset, and the combined dataset to examine differences in growth between the temperate North Pacific and the tropical and subtropical WCPO.

2.2 Approaches to address spatial sampling bias in growth estimation

Within MFCL, the growth curve is estimated from CAAL data, and the contribution of each region to the estimate is determined by the number of CAAL observations from that region. When the geographic composition of the CAAL dataset does not reflect the actual distribution of the stock, regions with high sampling effort but low abundance will disproportionately influence the estimated growth curve. The Japanese and SPC otolith datasets were collected independently, and their relative sample sizes reflect the respective sampling programs rather than regional stock abundance. Because BET growth parameters differ markedly between the temperate North Pacific and the tropical WCPO, combining the two datasets without accounting for regional abundance can produce a biased growth estimate. To address this, we propose two approaches that weight the contribution of CAAL data from each region in proportion to its relative abundance, using standardized Japanese longline CPUE as a proxy for regional stock distribution.

2.2.1 Standardized CPUE

We standardized Japanese longline CPUE for BET using a spatiotemporal model implemented in the sdmTMB R package (Anderson et al. 2022), following the approach described in Xu et al. (2024). Catch and effort data from Japanese longline operations in the WCPO (1979–2024) were aggregated by vessel to the 1°×1° grid and quarter. To ensure adequate data coverage, we retained vessels with at least 40 quarterly observations and grid cells with at least 20 quarterly observations.

The model consists of two components fitted jointly. The first component models the probability of a positive catch (encounter rate) with a binomial distribution and a logit link, given by

$$logit\, p_{s,t} = \beta_t + f\, HBF_{s,t} + u_v + \omega_s^{(1)} + \varepsilon_{s,t}^{(1)}$$

The second component models the expected catch rate conditional on a positive set with a lognormal distribution, given by

$$log\, r_{s,t} = \beta_t + f\, HBF_{s,t} + u_v + \omega_s^{(2)} + \varepsilon_{s,t}^{(2)} + log\, H_{s,t}$$

In both components, $\beta_t$ is a year-quarter fixed effect, *f*(HBF) is a thin-plate regression spline (*k* = 3) for hooks between floats that accounts for gear configuration effects on catchability, $u_v$ is a vessel-level random intercept, $\omega_s$ is a stationary spatial random field approximated via the SPDE method (Lindgren et al. 2011), $\varepsilon_{s,t}$ is a spatiotemporal random field with AR(1) temporal structure, and $H_{s,t}$ is the number of hooks, included as an offset in the positive catch

component. The combined CPUE at location *s* and quarter *t*, expressed per 1,000 hooks, is given by

$$CPUE_{s,t} = p_{s,t} \times r_{s,t} \times 1{,}000$$

Predictions were generated on a regular 1°×1° grid at the median observed HBF, excluding the vessel random effect. The predicted CPUE values were mean-centered by dividing by the global mean across all grid cells and quarters.

### 2.2.2 Approach 1: CPUE-proportional resampling

For each CAAL observation, we assigned a resampling weight proportional to the standardized CPUE at the corresponding 1°×1° grid cell and quarter. We then drew B = 200 bootstrap resamples of size 1,000 with replacement using these weights. A VB growth model was fitted to each resample. The resample with the estimated closest to the median Linf across all bootstrap iterations was designated as the representative CPUE-weighted growth curve. The 95% bootstrap confidence intervals for Linf and k were derived from the 2.5th and 97.5th percentiles of the bootstrap distributions.

### 2.2.3 Approach 2: Regional ESS scalars

This approach adjusts the contribution of CAAL data from each model region within the MFCL growth likelihood by scaling the observed sample size. We first computed the time-averaged standardized CPUE for each 1°×1° grid cell ($I_k$) and then calculated the mean CPUE for each model region ($\bar{I}_r$) as the average of $I_k$ across all cells within that region. The regional scalar $\lambda_r$ was defined as

$$\lambda_r = \frac{\bar{I}_r}{\bar{I}}$$

where $\bar{I}$ is the mean of $\bar{I}_r$ across all model regions. Within MFCL, the effective sample size (ESS) for CAAL data in region *r* ($\varepsilon_{ir}$) is modified as

$$\varepsilon_{ir} = p_{CAAL} \times \lambda_r$$

where $p_{CAAL}$ is the observed sample size used in the base assessment. Regions with $\lambda_r > 1$ contribute more to the estimated growth curve than in the base case, and regions with $\lambda_r < 1$ contribute less. We computed λ_r values based on the five-region spatial structure proposed for the 2026 BET stock assessment, with region boundaries shown in Figure 3.

## Results

### 3.1 Growth curves by dataset

The FRA and SPC datasets covered complementary size ranges and geographic regions (Figures 1, 2). The FRA BET samples (N = 443) were collected from the subtropical and temperate North Pacific (10°N–37°N, 128°E–158°W) with fork lengths of 60–177 cm. The SPC BET samples (N = 1,644) were collected from the tropical and subtropical WCPO (41°S–31°N, 120°E–123°W) and covered a broader size range (14–183 cm). For YFT, the FRA dataset (N = 141) covered 10°N–39°N with fork lengths of 60–145 cm, while the SPC dataset (N = 1,832) covered fork lengths of 14–174 cm from tropical WCPO waters. The combined datasets comprised 2,087 BET and 1,973 YFT samples.

The estimated VB growth curves showed difference between the FRA and SPC datasets, particularly for BET (Figure 1; Table 1). The estimated parameters were Linf = 178.0 cm and $k$ = 0.296 for the FRA dataset, and Linf = 150.0 cm and $k$ = 0.384 for the SPC dataset. At age 1, the FRA curve predicted a fork length of 58.9 cm compared to 64.3 cm from the SPC curve. Then, the two curves crossed at approximately age 2.5 years (approximately 103 cm), after which the FRA growth curve predicted greater lengths. By age 7, the FRA curve predicted 157.8 cm compared to 141.4 cm from the SPC curve. The asymptotic lengths differed by 28.0 cm (178.0 cm vs. 150.0 cm). The curve fitted to the combined dataset fell between the two regional curves (Linf = 157.5 cm, $k$ = 0.345).

For YFT, the estimated parameters were Linf = 131.7 cm and $k$ = 0.714 for the FRA dataset, and Linf = 147.0 cm and $k$ = 0.461 for the SPC dataset (Figure 2; Table 1). At age 1, the FRA curve predicted 58.9 cm compared to 64.0 cm from the SPC curve. Unlike BET, the FRA growth curve for YFT did not overtake the SPC curve at any age. The FRA parameter estimates, however, are not well constrained by the available data: only 13 of 141 FRA YFT samples (9%) were older than 5 years, which makes the parameter estimates unreliable. Given this uncertainty, differences between the FRA and SPC growth curves for YFT at older ages cannot be reliably assessed from the current dataset.

The regional difference in growth was greater for BET than for YFT. We therefore focus the subsequent analysis on BET.

### 3.2 CPUE-based weighting approaches for BET

The standardized Japanese longline CPUE for BET showed spatially variable distribution across the WCPO (Figure 3). CPUE was highest in the equatorial Pacific (R3 and R4), intermediate in the archipelagic waters region (R2), and lowest in the southern Pacific (R5) and northern Pacific (R1).

Using the CPUE-proportional resampling bootstrap, the estimated parameters for the CPUE-weighted combination (G_boot) were Linf = 162.0 cm (95% bootstrap CI: 158.6–165.6 cm) and $k$ = 0.323 (95% CI: 0.303–0.344; Figure 4). The unweighted curve fitted to the combined dataset (G_mixed) had Linf = 157.9 cm and $k$ = 0.344. G_boot had a higher asymptotic length and slower growth rate than G_mixed, reflecting the CPUE distribution of

Japanese longline operations. The FRA-only curve (G_temp: Linf = 178.0 cm) and SPC-only curve (G_trop: Linf = 150.2 cm) differed by 27.8 cm in asymptotic length. G_boot fell between these two curves at 162.0 cm, shifted toward higher Linf relative to G_mixed.

The regional ESS scalars ($\lambda_r$) derived from 1°×1° time-averaged CPUE ranged from 0.61 (R5) to 1.33 (R4) across the five BET model regions (Figure 5; Table 2). For R3 and R4, $\lambda_r$ was above 1.0, meaning CAAL data from these regions would be upweighted in the MFCL growth likelihood relative to an equal-weight scenario. R2 (1.01) was approximately equal to the mean. In contrast, $\lambda_r$ was below 1.0 for the northern Pacific (R1 = 0.83) and southern Pacific (R5 = 0.61). Applying these scalars to the MFCL CAAL likelihood would upweight data from high-CPUE tropical regions and downweight data from lower-CPUE northern and southern regions.

## Discussion

This study expanded the spatial coverage of CAAL data available for WCPO BET and YFT assessments and proposed two approaches to account for regional differences in sample availability when estimating growth within MFCL. The newly incorporated otolith samples from the temperate North Pacific revealed substantial differences in BET growth relative to existing datasets mainly from the tropical region, highlighting the potential influence of spatial sampling composition on growth estimation. Because MFCL assumes a single growth curve across the assessment domain, these results suggest that the geographic composition of CAAL data can affect the growth curve estimated by the model. The CPUE-based weighting approaches presented here provide a practical framework for incorporating regional abundance into growth estimation and may help improve the representativeness of growth curves used in the assessment model for BET.

Our results demonstrated that growth differed substantially between the temperate North Pacific and the tropical WCPO, particularly for BET. Fish in the tropics grew faster at young ages, while fish from the temperate North Pacific reached greater asymptotic lengths. A previous study reported the longitudinal variation in BET growth across the WCPO, with fish in the eastern areas tending to be larger at age than those in the central Pacific (Farley et al. 2017). However, the available otolith dataset at that time was concentrated in tropical waters, limiting the opportunity to fully characterize the latitudinal variation. By incorporating 443 additional BET otoliths from the temperate North Pacific, the study provided further evidence that BET growth can vary between temperate and tropical regions. Several mechanisms may account for the observed regional differences in BET growth. Temperature is the most commonly cited driver of spatial growth variation in fish. In the VB bioenergetics framework, lower ambient temperatures reduce catabolic rates, which can result in slower growth at young ages but greater asymptotic body size (Lorenzen 2016). The pattern observed here, with lower *k* and higher Linf in the temperate North Pacific relative to the tropical WCPO, is consistent with this temperature effect. Differences in prey availability and

foraging ecology between the productive temperate and oligotrophic tropical Pacific may also contribute. Further studies are required to examine the potential mechanism.

The assumption of spatially invariant growth is increasingly recognized as a potential source of bias in integrated assessment models. When growth parameters differ substantially across a stock's range, a single growth curve may misrepresent the population age structure, resulting in biased estimates of abundance and biomass. Punt et al. (2015) used simulation to show that non-spatial assessment configurations gave 10–35% median absolute relative error in spawning biomass when spatial heterogeneity in growth and fishing mortality was present. Correa et al. (2021) extended this analysis to integrated assessment models and demonstrated that ignoring spatial variation in growth led to biases in spawning stock biomass of 30–70% under scenarios where fishing effort was unevenly distributed across regions with differing growth characteristics. Although both studies used non-tuna species, the findings indicate that integrated assessment models are sensitive to growth assumptions when fish populations exhibit spatial structure in growth. Allowing assessment models to estimate region-specific growth parameters would provide the most direct solution, but implementing such an extension within MFCL is not currently feasible. However, this could be considered as an important feature to build into next generation tuna stock assessment software.

The two approaches proposed in this study offer a practical means of reducing growth estimation bias within the existing framework by weighting CAAL data from each region in proportion to its relative abundance. Both approaches use Japanese longline CPUE as a proxy for regional BET abundance to adjust the contribution of each dataset to growth estimation within MFCL. Approach 1 modifies the input data before model fitting and is therefore applicable to any stock assessment framework, while Approach 2 is implemented directly within the MFCL likelihood and preserves the full sample size for variance estimation. Under Approach 1, CPUE-proportional resampling shifted the combined growth curve towards higher Linf relative to the unweighted combination, reflecting the underlying CPUE distribution. This finding is consistent with Bolser et al. (2018) that showed that sample composition strongly influences which growth curve is estimated from fishery-dependent data and that statistically superior model fit does not guarantee a biologically representative estimate. Under Approach 2, the equatorial Pacific regions (R3 and R4), where $\lambda r$ exceeded 1.0, would contribute more to the estimated growth curve within MFCL, while the northern Pacific (R1) and southern Pacific (R5), where $\lambda r$ fell below 1.0, would contribute less. Peatman et al. (2025) reached a similar conclusion that spatially proportional otolith sampling reduces bias in MFCL-based growth estimation for BET and skipjack, providing additional support for the weighting concept adopted here.

There are several limitations in this study. The proposed approaches rely on Japanese longline CPUE as a proxy for regional relative abundance, which requires that standardized CPUE is proportional to local stock density across regions. This assumption is valid if CPUE reflects true stock abundance. However, CPUE can also reflect the distribution of fishing effort

as well as abundance, and areas not covered by Japanese longline operations are excluded from the analysis. Future improvement is needed by including other fisheries to reduce the bias rather than focusing on particular fishery. In addition, the analysis focused on BET because the FRA YFT dataset lacked sufficient representation of older fish to draw reliable conclusions about growth at older ages. A spatially stratified sampling program targeting older YFT in tropical waters, as recommended by Peatman et al. (2025), would substantially improve the reliability of YFT growth estimates. For BET, continued otolith collection from both the temperate North Pacific and the equatorial WCPO, with sampling proportional to regional catch composition, would reduce dependence on post-hoc reweighting.

## References


Anderson SC, Ward EJ, English PA, Barnett LAK (2022) sdmTMB: an R package for fast, flexible, and user-friendly generalized linear mixed effects models with spatial and spatiotemporal random fields. bioRxiv 2022.03.24.485545. https://doi.org/10.1101/2022.03.24.485545

Bolser DG, Grüss A, Lopez MA, Reed EM, Mascareñas-Osorio I, Erisman BE (2018) The influence of sample distribution on growth model output for a highly-exploited marine fish, the Gulf Corvina (Cynoscion othonopterus). PeerJ 6:e5582.

Correa GM, McGilliard CR, Ciannelli L, Fuentes C (2021) Spatial and temporal variability in somatic growth in fisheries stock assessment models: evaluating the consequences of misspecification. ICES Journal of Marine Science 78(5): 1872–1886. https://doi.org/10.1093/icesjms/fsab096

Day J, Magnusson A, Teears T, Hampton J, Davies N, Castillo Jordán C, Peatman T, Scott R, Scutt Phillips J, McKechnie S, Scott F, Yao N, Natadra R, Pilling G, Williams P, Hamer P (2023) Stock assessment of bigeye tuna in the western and central Pacific Ocean: 2023. WCPFC-SC19-2023/SA-WP-05.

Farley JH, Eveson JP, Krusic-Golub K, Clear NP, Sanchez C, Nicol SJ (2025) Jesstimation: A novel approach for estimating more accurate fish ages from otolith zone counts and measurements. Fisheries Research 288: 107463.

Farley JH, Kopf RK, Williams AJ, Clear NP, Davies CR (2020) Age and growth of yellowfin and bigeye tuna in the western and central Pacific Ocean. WCPFC-SC16-2020/SA-WP-02.

Farley JH, Williams AJ, Davies CR, Clear NP, Nicol SJ (2017) Demographic structure and recruitment variability of bigeye tuna in the western and central Pacific Ocean. WCPFC-SC13-2017/SA-WP-01.

Lindgren F, Rue H, Lindström J (2011) An explicit link between Gaussian fields and Gaussian Markov random fields: the stochastic partial differential equation approach. Journal of the Royal Statistical Society Series B 73(4): 423–498.

Lorenzen K (2016) Toward a new paradigm for growth modeling in fisheries stock assessments: embracing plasticity and its consequences. Fisheries Research 180: 4–22.

Magnusson A, Day J, Teears T, Hampton J, Davies N, Castillo Jordán C, Peatman T, Scott R, Scutt Phillips J, McKechnie S, Scott F, Yao N, Natadra R, Pilling G, Williams P, Hamer P (2023) Stock assessment of yellowfin tuna in the western and central Pacific Ocean: 2023. WCPFC-SC19-2023/SA-WP-04.

Peatman T, Scutt Phillips J, Potts J, Nicol S (2025) WCPFC Projects 117 and 118: The development of biological sampling plans for tuna and billfish. WCPFC-SC21-2025/SA-WP-15.

Punt AE, Haddon M, Tuck GN (2015) Which assessment configurations perform best in the face of spatial heterogeneity in fishing mortality, growth and recruitment? A case study based on pink ling in Australia. Fisheries Research 168: 85–99.

Xu W, Hamer P, Davies N, Hampton J (2024) Standardization of Japanese longline CPUE for bigeye tuna in the western and central Pacific Ocean. WCPFC-SC20-2024/SA-IP-XX. [Citation to be confirmed by author]

**Tables**

Table 1. Von Bertalanffy growth parameters estimated from age-at-length data by species and dataset. SE = standard error.

| Species | Dataset | N | Linf (cm) | SE | k ($yr^{-1}$) | SE | $t_0$ (yr) | SE |
|---|---|---|---|---|---|---|---|---|
| BET | FRA | 443 | 178.0 | 2.51 | 0.296 | 0.015 | −0.356 | 0.081 |
| BET | SPC | 1,644 | 150.0 | 0.76 | 0.384 | 0.007 | −0.456 | 0.020 |
| BET | Combined | 2,087 | 157.5 | 0.90 | 0.345 | 0.006 | −0.498 | 0.024 |
| YFT | FRA | 141 | 131.7 | 3.09 | 0.714 | 0.064 | 0.170 | 0.115 |
| YFT | SPC | 1,832 | 147.0 | 0.74 | 0.461 | 0.007 | −0.240 | 0.014 |
| YFT | Combined | 1,973 | 146.6 | 0.76 | 0.464 | 0.007 | −0.237 | 0.014 |

Table 2. Region-specific ESS scalars ($\lambda_r$) for the five BET model regions derived from 1°×1° time-averaged standardized Japanese longline CPUE. $\bar{I}_r$ = regional mean CPUE.

| Region | $\bar{I}_r$ | $\lambda_r$ |
|---|---|---|
| R1 | 0.948 | 0.827 |
| R2 | 1.155 | 1.009 |
| R3 | 1.404 | 1.226 |
| R4 | 1.523 | 1.330 |
| R5 | 0.697 | 0.608 |

**Figures**

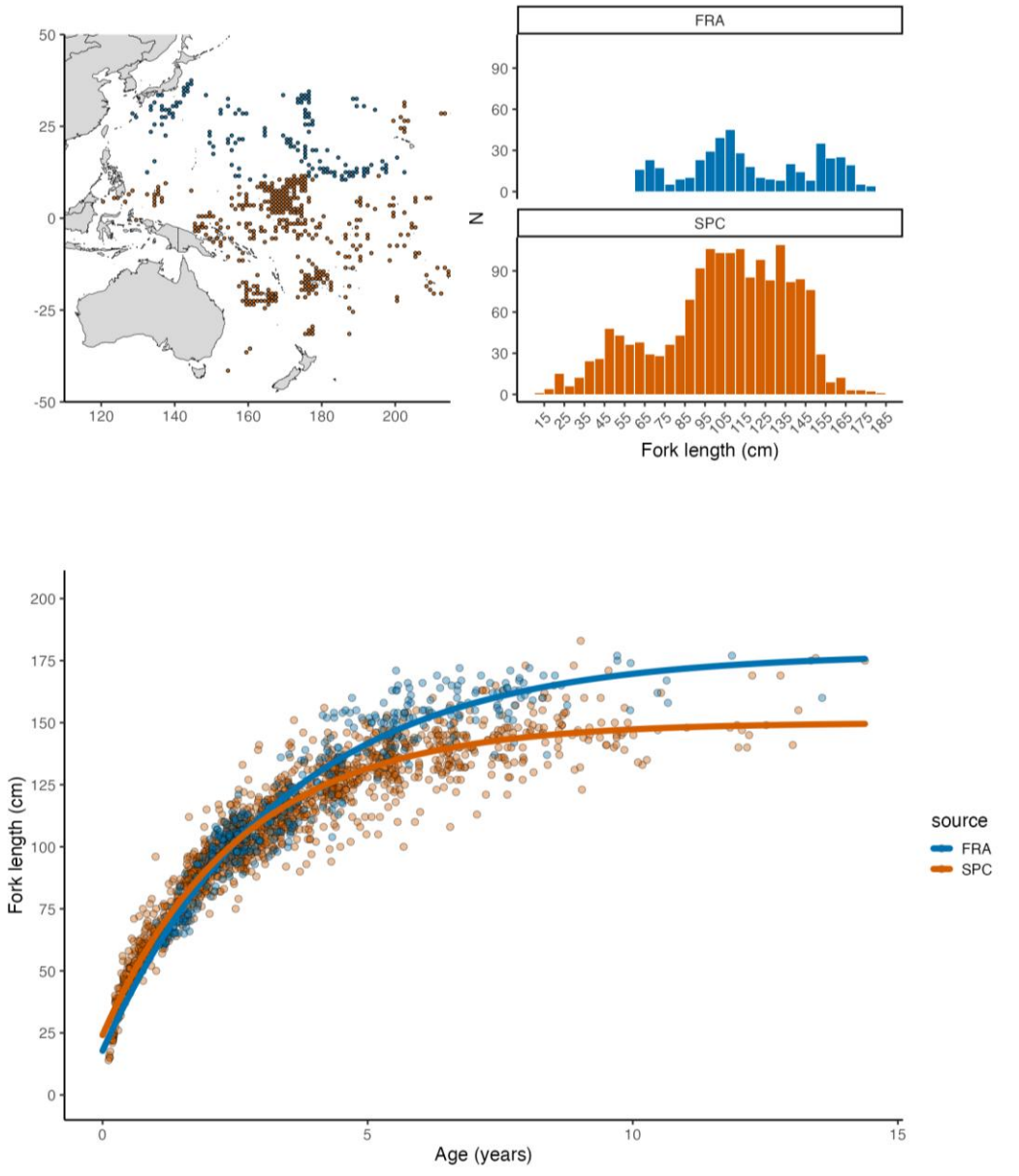


Figure 1. Age-at-length data and estimated von Bertalanffy growth curves for BET from the FRA (temperate North Pacific) and SPC (tropical and subtropical WCPO) datasets.

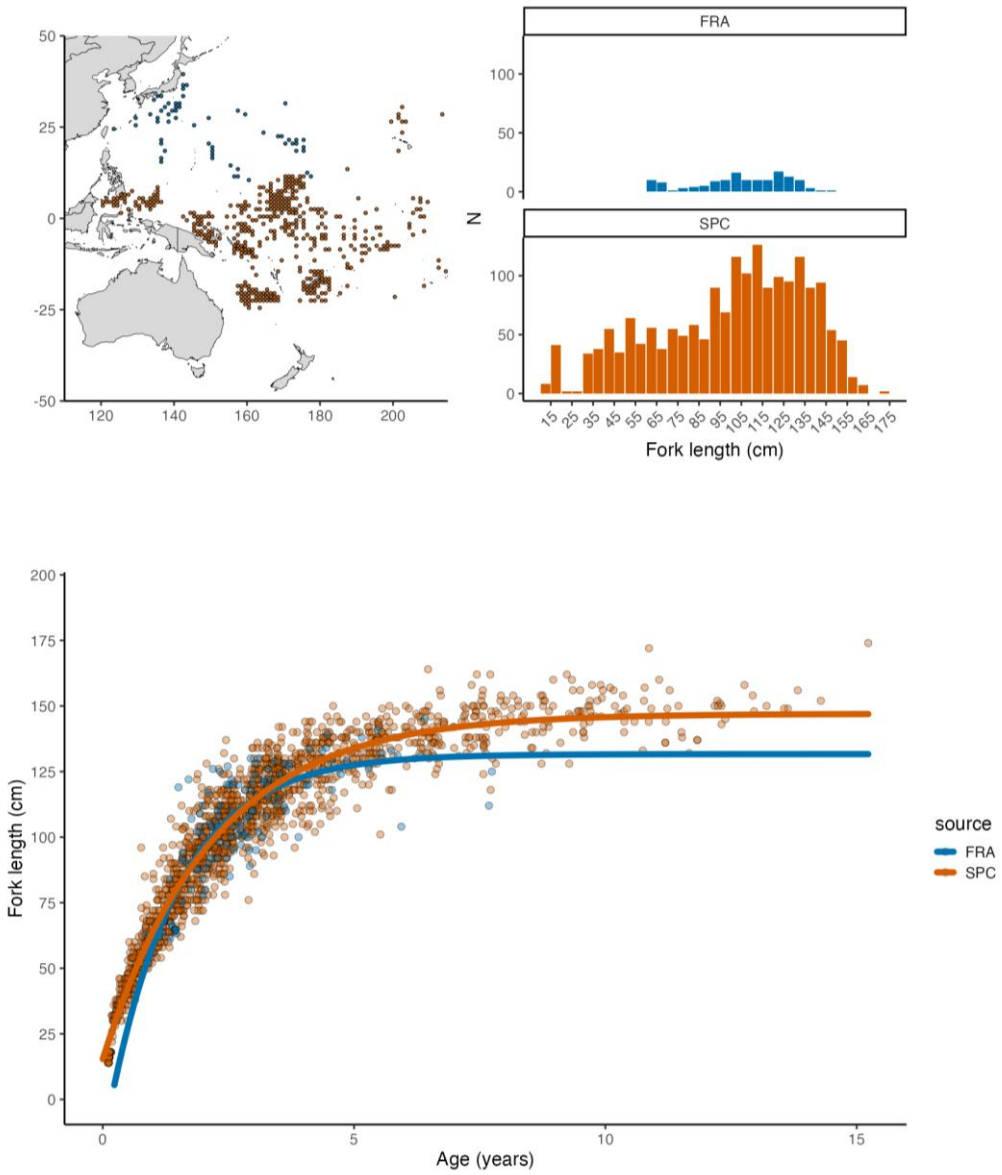


**Figure 2.** Age-at-length data and estimated von Bertalanffy growth curves for yellowfin tuna (YFT) from the FRA (temperate North Pacific) and SPC (tropical and subtropical WCPO) datasets.

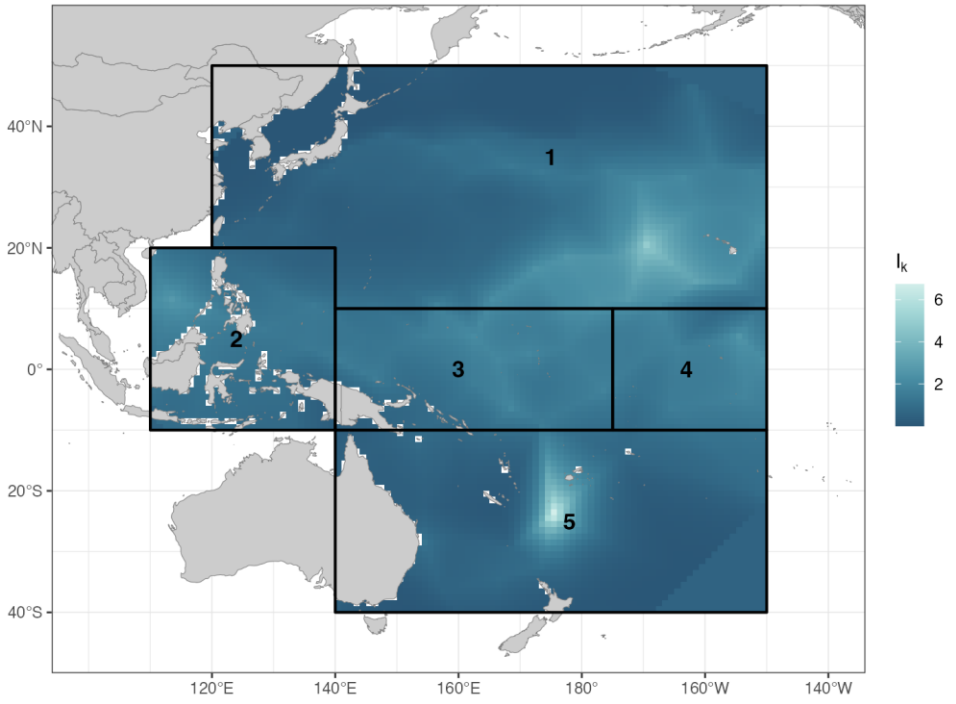


**Figure 3.** Mean standardized Japanese longline CPUE for BET across the 1°×1° grid, estimated using the spatiotemporal delta model implemented in sdmTMB. Values are mean-centered relative to the grand mean across all grid cells and quarters (1979–2024). Black lines indicate the boundaries of the five BET model regions.

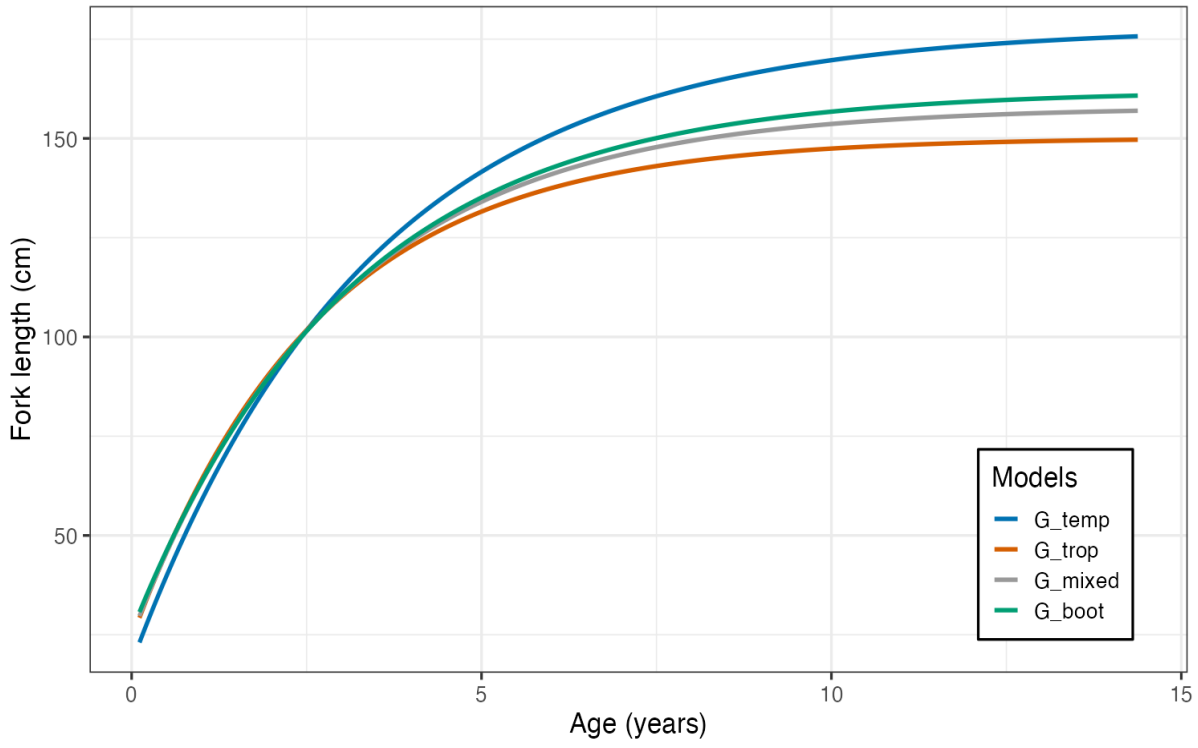

**Figure 4.** Von Bertalanffy growth curves for BET estimated from the CPUE-proportional bootstrap resample (G_boot), the unweighted combined dataset (G_mixed), the FRA-only dataset (G_temp), and the SPC-only dataset (G_trop).

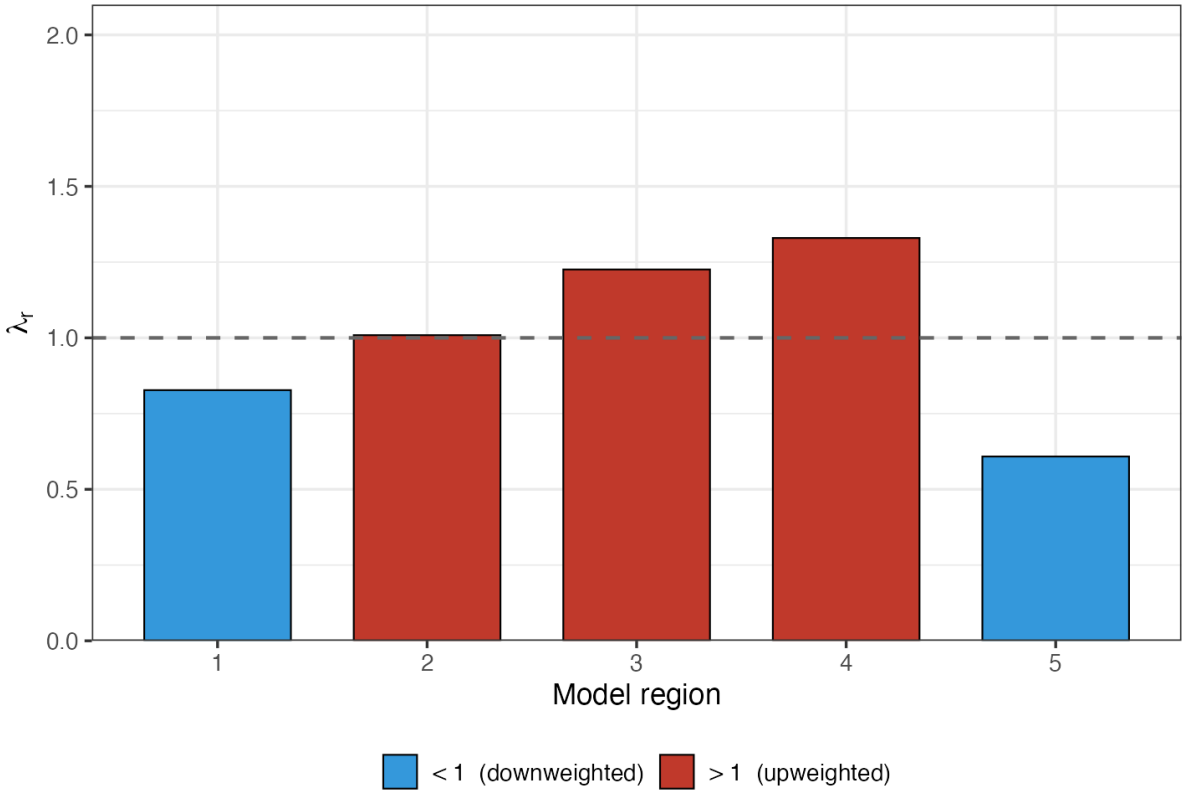


Figure 5. Region-specific ESS scalars (λr) for the five BET model regions derived from 1°×1° time-averaged standardized Japanese longline CPUE. Regions with λr > 1 contribute more to the MFCL growth likelihood than in the base assessment; regions with λr < 1 contribute less.